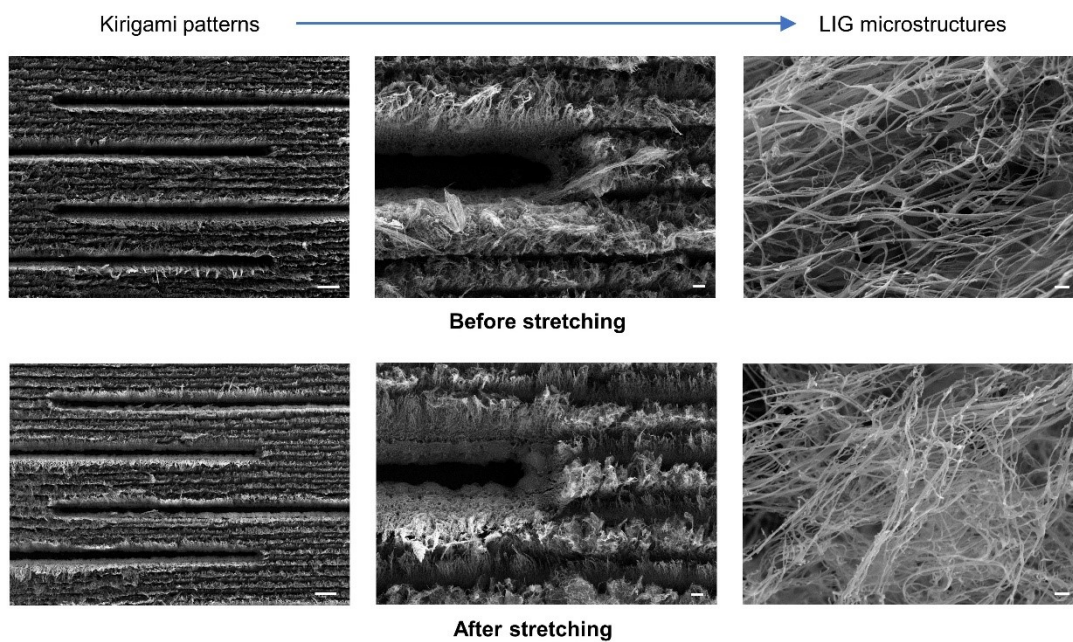


### Supplementary information



**Fig. S1** SEM images of LIG with kirigami pattern (scale bar - left: 200 μm; middle: 20 μm; right: 600 nm).

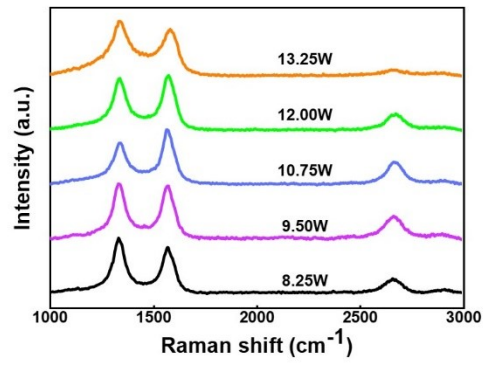
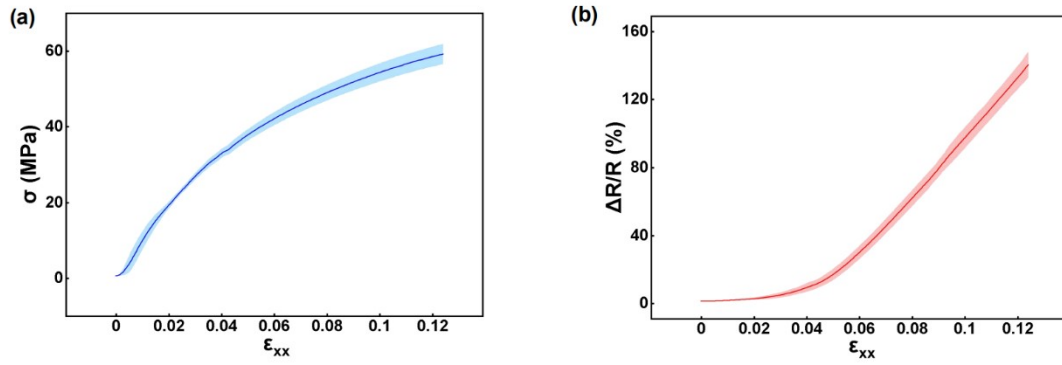
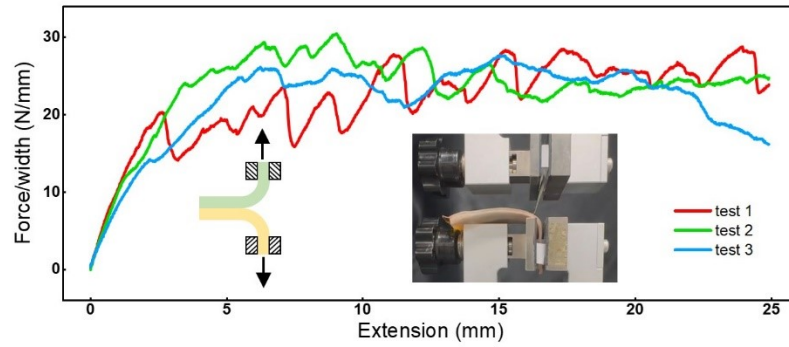


Fig. S2 Raman spectrum of LIG.



**Fig. S3** Mechanical and electrical test of LIG on a continuous PI film. The gage length and gage width of the dog bone specimen are 20 mm and 5 mm, respectively. (a) Stress – strain relationship of LIG (without kirigami patterns) fabricated by 10.75 W laser power. (b) Resistance variation – strain relationship of LIG fabricated by 10.75 W laser power.



**Fig. S4** Adhesion property of the heater.

A T-peeling test is carried out to verify that the LIG heaters have good adhesion to skin. Since porcine skin closely resembles the surface property of human skin, we chose porcine skin with the same size as the unidirectional heater to be the model for heater-skin bonding testing.<sup>1</sup> The force/width curve for adhesion between the heater and porcine skin is shown as follows. The average adhesion energy is  $23.93 \text{ Jm}^{-2}$ , which is comparable with silicone-based adhesives for long-term skin application with the adhesion energy ranging from  $0.5 \text{ Jm}^{-2}$  to  $22.5 \text{ Jm}^{-2}$ ,<sup>2</sup> indicating a good adhesion to skin.

1 B. Ying, R. Z. Chen, R. Zuo, J. Li and X. Liu, *Adv. Funct. Mater.*, 2021, 2104665.

2 L. Liu, K. Kuffel, D. K. Scott, G. Constantinescu, H.-J. Chung and J. Rieger, *Biomed. Phys. Eng. Express.*, 2017, 4, 015004.

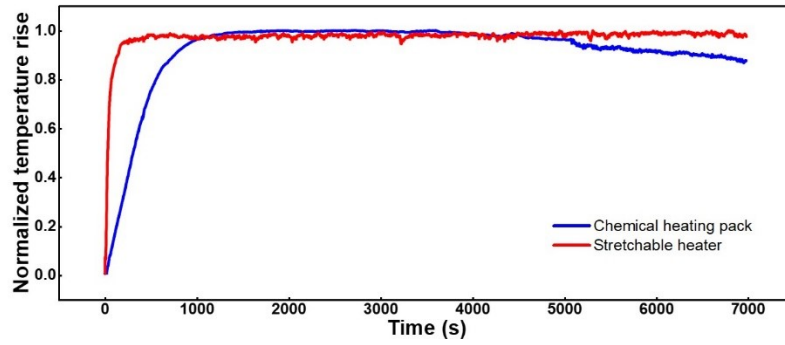


**Fig. S5** Temperature response of the chemical heating pack.

We conducted an experiment to measure the temperature response of a conventional chemical heating pack (160 mm × 120 mm, Pengyi Co.), which generates heat through an oxidation reaction between oxygen and ferrous powder. The temperature measurement with K type thermocouple commenced immediately after the heating pack was removed from its sealed packaging. Our findings revealed that it takes approximately 760 seconds for the heating pack to achieve 90% of its maximum temperature rise.

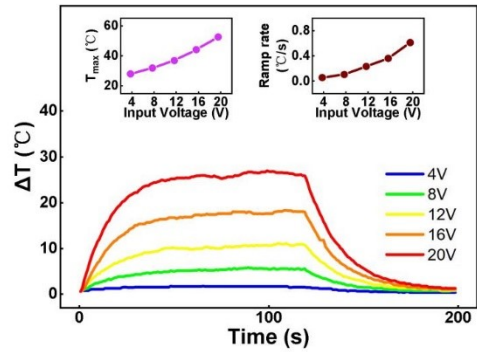


**Fig. S6** Transient temperature response under different input voltage (multidirectional heater,  $r_2=0.5$ , strain = 0. Insets: maximum  $\Delta T$  and ramp rate at different input voltage).

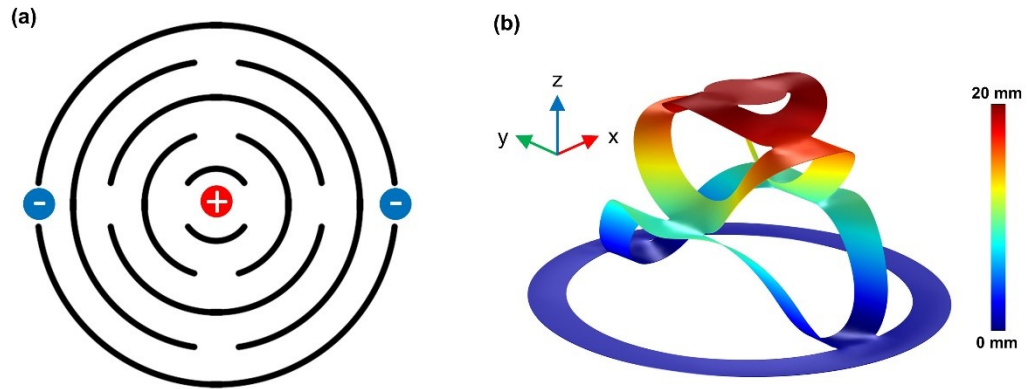


**Fig. S7** Concentric annulus kirigami structure. (a) Schematic diagram with cathode represented by blue dots and anode represented by red dot. (b) FEA result of the concentric annulus kirigami structure stretched in z direction.

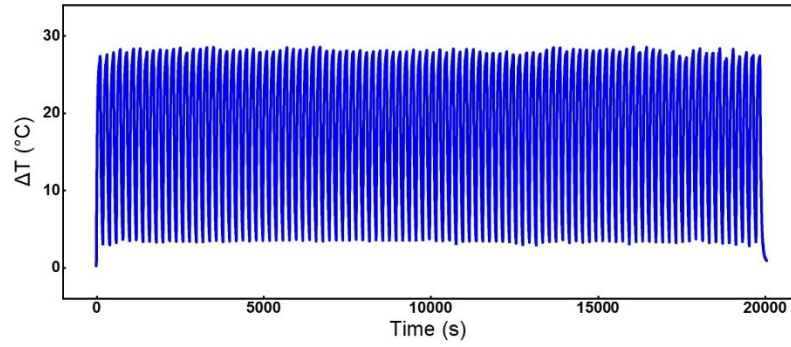


**Fig. S8** 100 power on/off cycles.

To assess the electrothermal stability, we conducted a test involving continuous monitoring of the heating temperature of a representative unidirectional LIG heater in 100 power on/off cycles. In each cycle, the heater was subjected to an input DC voltage of 10 V for the first 120 seconds, followed by a power-off phase lasting 80 seconds. The key finding from this test is the consistent maximum temperature rise in each cycle, maintained at around 28 °C. This consistency in temperature elevation across numerous cycles is a strong indicator of the heater's electrothermal stability. It demonstrates the heater's ability to reliably produce and maintain the desired thermal output over repeated use, without significant fluctuations or degradation in performance.

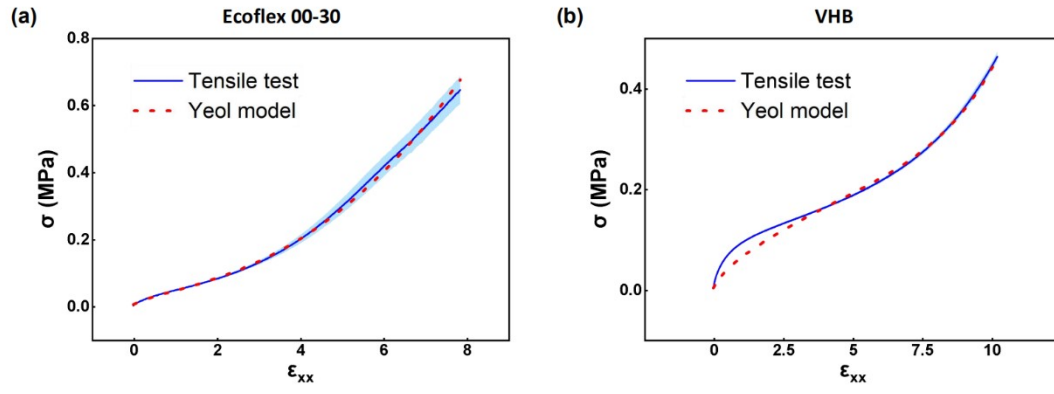
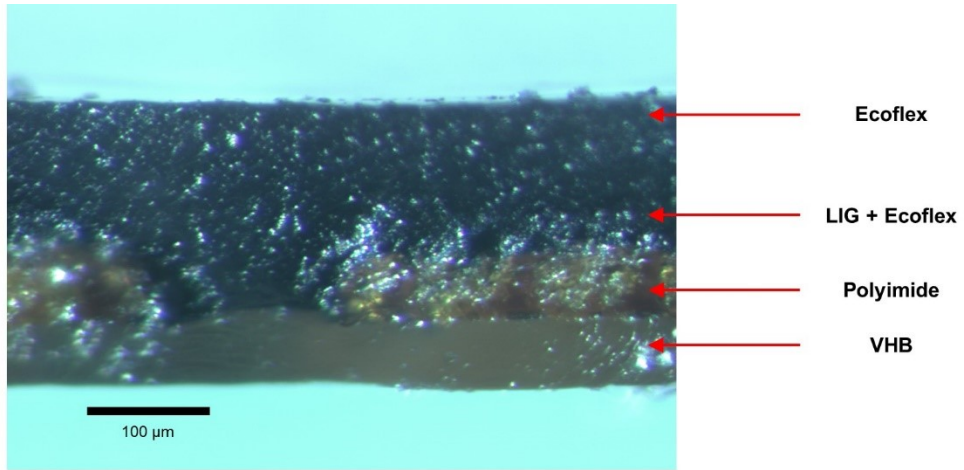


Fig. S9 Hyperelastic model of (a) Ecoflex and (b) VHB ( $\sigma$ - $\lambda$ ).



**Fig. S10** Cross section of the unidirectional heater.